Supporting Information

Paliwal et al. 10.1073/pnas.1004302107

SI Text

A. List of Surfactants Used in the Study. A set of 19 representative surfactants was chosen and classified in four groups according to the surfactant's head group chemistries: (*i*) anionic surfactants [sodium lauryl sulfate (SLS), sodium laureth sulfate (SLA), sodium tridecyl phosphate (TDP), sodium deoxycholate (SDC), sodium decanoyl sarcosinate (NDS), sodium lauroyl sarcosinate (NLS), sodium palmitoyl sarcosinate (NPS)]; (*ii*) cationic surfactants [octyl trimethyl ammonium chloride (OTAB), dodecyl trimethyl ammonium chloride (DDTAB), tetradecyl trimethyl ammonium chloride (TTAB)]; (*iii*) zwitterionic surfactants [3-[(3-Cholamidopropyl) dimethyl ammonio]1-propane sulfonate (CHAPS), 3-(Decyl dimethyl ammonio) propane sulfonate (DPS), 3-(Dodecyl dimethyl ammonio) propane sulfonate (DDPS)); (*iv*) nonionic surfactants [polyethylene glycol dodecyl ether (B30), polyoxyethylene 23-lauryl ether (B35), polyoxyethylene 10-cetyl ether (B56), polyoxyethylene 2-stearyl ether (B72), polyethylene glycol oleyl ether (B93), nonylphenol polyethylene glycol ether (NP9)]. TDP, SDC, NLS, NPS, OTAB, DDTAB, TTAB, CHAPS, DPS, DDPS, B35, B56, B72, B93 and NP9 were procured from Sigma-Aldrich. NDS and B30 were procured from TCI America. SLS was procured from Fisher Scientific. NPS and SLA were generously gifted by Barnet Products Corp. (Englewood Cliffs, NJ) and Chemron Corp. (Paso Robles, CA), respectively.

B. Synergistic Behavior of Surfactant Formulations. To gauge the unexpected interplay between surfactants with differing properties, a Synergy Index (S) for each surfactant formulation was calculated:

$$S = \frac{B^X_{A+B}}{(B^X_A + B^X_B)/2},$$

where B^X_{A+B} is the bioactivity of a formulation obtained by combining surfactants A and B at a total concentration of $X\%$ (wt/vol), and B^X_A and B^X_B are bioactivities of surfactant A and B, respectively, at a concentration of $X\%$ (wt/vol). In parallel to the discovery of synergistic formulations ($S > 1$), a significant number of formulations also showed anergy ($S < 1$). Synergy Indices of the binary formulations, when fitted to Gaussian distribution statistics, confirmed that the probability of finding surfactant formulations with higher synergy potential progressively decreases with increasing Synergy Index (Fig. S1 *A* and *B*). Our data demonstrate the existence of such rare and uniquely synergistic surfactant formulations for preserving bioactivity.

C. Enhanced Sampling of Functional Molecules by 0.5% (wt/vol) DPS-B30 Formulation. Increased sampling of functional tissue constituents by STAMP (**S**urfactant-based **T**issue **A**cquisition for **M**olecular **P**rofiling) is a compounded result of the unique ability of 3-(Decyl dimethyl ammonio) propane sulfonate and polyethylene glycol dodecyl ether (DPS-B30) to solubilize molecules from tough tissue assemblies as well as to retain molecular bioactivity during sonication stress. We studied both of these unique characteristics.

Solubilization of tissues is mediated primarily by surfactants. Ultrasound contributes to the process by enhancing the penetration and dispersion of surfactants in the skin. The ability of ultrasound to enhance the penetration and dispersion of surfactants in the skin has already been demonstrated, primarily using SLS as a surfactant (1). The effect of surfactant and ultrasound on skin, however, is highly localized, leading to the formation of localized transport regions (LTRs) (2). Our studies showed that application of ultrasound to skin with 0.5% (wt/vol) DPS-B30 leads to a 3-fold enhancement of area of LTRs compared to that from 1% (wt/vol) SLS (Fig. S4*A*). This suggests increased access of DPS-B30 to the tissue for sampling biomolecules. Additionally, we observed that DPS-B30-ultrasound combination yielded about 3-fold higher proportion of soluble protein in the sample compared to that yielded by SLS-ultrasound combination (Fig. S4*B*). Collectively, these results indicate that for a given ultrasound condition, DPS-B30 formulation provides dramatically higher recovery of solubilized protein compared to that by SLS.

The benefits of DPS-B30 are further escalated by its ability to preserve the protein structure. Unlike SLS, it prevents protein denaturation on its own. In addition, it also protects proteins against ultrasound-induced denaturation. Dynamic light scattering and FTIR spectroscopy studies were performed to get insights into this behavior. Lysozyme was used a model protein because of its availability in pure and large quantities, and well-characterized behavior in aqueous solution. Light scattering studies revealed that lysozyme, when solubilized in saline, rapidly forms large aggregates when subjected to ultrasound (aggregate size of 229.5 ± 72 nm compared to native size of 5.4 ± 0.01 nm; Fig. S5*A*). In contrast, lysozyme prepared in 0.5% (wt/vol) DPS-B30 surfactant formulation did not aggregate when exposed to ultrasound. Direct measurement of lysozyme bioactivity (Fig. 2*C*) and FTIR studies (Fig. S5*B*) also confirmed these findings. A significant rearrangement of β-sheets (from intramolecular to intermolecular β-sheets) was observed after sonication of lysozyme prepared in saline. Increased content of intermolecular β-sheets is the most prominent change in the secondary structure of aggregated proteins and is commonly found in proteins subjected to thermal, chemical, or physical stress (3, 4). Rearrangement of β-sheets to intermolecular conformation without grossly changing the secondary protein structure is expected. Physical shearing, similar to cavitation-induced forces experienced by protein under ultrasound exposure, has been shown to disrupt protein's native fold but leave secondary structural elements intact and thereby enhance intermolecular interactions and aggregation (5). Notably, formation of aggregates and increase in the intermolecular β-sheets for several proteins (including lysozyme) subjected to low-frequency ultrasound (as used in STAMP) have been previously reported (6). Consistent with the absence of aggregates (found by light scattering), no change in the intermolecular β-sheet content was observed when DPS-B30 surfactant formulation was added during sonication of lysozyme (Fig. S5*B*). These results demonstrate the ability of DPS-B30 to prevent protein aggregation, possibly by stabilizing their transient unfolded state and increasing the kinetic rates of protein refolding.

The experiments reveal that DPS-B30 provides three beneficial contributions; biomolecular recovery from larger skin area, higher fraction of solubilized proteins and protection of proteins against denaturation. Collectively, they allow high recovery of functional proteins and other biomolecules from the skin.

D. Methods. ***In vitro tissue solubilization protocol.*** Porcine skin was used as a model tissue in these experiments. Skin was procured in frozen form from Lampire Biological Laboratories Inc. Skin was stored at −70 °C until the experiment. Two hours before the experiment, skin was thawed at room temperature and cut into small pieces (2.5 cm × 2.5 cm). Skin pieces stripped off from subcutaneous fat and with no visible imperfections such as scratches

and abrasions were used. Solubilization experiment was carried out by mounting the skin piece on a Franz diffusion cell assembly (tissue exposure area of 1.77 cm^2; Permegear). The receiver chamber of the diffusion cell was filled with PBS and the donor chamber was filled with 1 mL of surfactant formulation as sampling buffer. This buffer also acted as the coupling fluid between the ultrasound transducer and the tissue. Solubilization was performed at room temperature with a 600-W probe sonicator (Sonics & Materials) operating at a frequency of 20 kHz. The ultrasound transducer was placed at a distance of 5 mm from the tissue surface and an ultrasonic intensity of 2.4 W/cm^2 at 50% duty cycle was applied for 3 min. Ultrasonic intensity was measured by using a calibrated hydrophone (detailed description in ref. 2). The sampling buffer, now containing solubilized tissue constituents, was aspirated and kept at −70 °C until analysis.

In vivo STAMP sampling protocol. A custom-made flanged chamber (skin exposure area of 1.33 cm^2) was adhered to the shaven skin area with a minimal amount of cyanoacrylate-based adhesive. The chamber was filled with 1.8 mL of 0.5% DPS-B30 surfactant formulation and ultrasound was applied by lowering the probe transducer in the chamber and keeping it to a distance of 5 mm from the skin surface. The breathing of animals required that we use a bigger chamber and larger sampling volume of 1.8 mL, compared to 1 mL for in vitro experiments, to ensure good contact of the ultrasound probe with the liquid.

ELISA protocol. All ELISA reagents were purchased from KPL. Immulon-2 U-bottom polystyrene plates purchased from Dynex Laboratories were coated with 100 μg chicken albumin (OVA) per well (1 mg/mL) in coating buffer for 1 h at room temperature. The plates were then blocked with nonfat milk-based blocking solution for 15 min. Test samples were generated by preincubating IgE antibody at 1 μg/mL with surfactant formulations for 1 h and loaded onto the ELISA plate. The plates were incubated for 1 h at room temperature and washed 3 times with wash buffer. The plates were then incubated with horseradish peroxidase-conjugated goat anti-mouse IgE antibody (2 μg/mL; catalog no. GE-90P-Z, ICL Inc.) for 1 h. The plates were washed 4 times with wash buffer and treated with ABTS two-component substrate system. The absorbance was read at 405 nm 5 min after mixing of substrate. For each surfactant formulation, the ELISA signal was corrected for nonspecific background activity, obtained by omitting addition of IgE antibody in the surfactant formulation.

Compatibility of leading surfactant formulation with ELISA. Several quantitative analytical techniques rely on unique protein-ligand interactions and demand a strong linear signal response over a wide range of analyte concentration. Surfactant-based additives such as 0.5% (wt/vol) Tween20 are typically used to facilitate protein-ligand interactions, avoid protein aggregation in samples, and reduce nonspecific assay signal. The compatibility of the leading surfactant formulation—0.5% (wt/vol) DPS-B30 (used in STAMP procedure) with ELISA-based protein assay was assessed. Fig. S6 demonstrates that DPS-B30 formulation was found to be highly compatible with IgE-OVA ELISA over a large analyte concentration range (IgE: 10–1,000 ng/mL), obviating the critical need for additives to enhance assay sensitivity. Additionally, we found that the solubilization potential of 0.5% (wt/vol) DPS-B30 for porcine skin (0.480 ± 0.116 mg/cm^2 of total protein) was significantly higher than 0.5% (wt/vol) Tween20 (0.045 ± 0.013 mg/cm^2). These combined results demonstrate that DPS-B30 formulation may provide an ideal tissue liquefaction medium that can interface well with existing analytical assays.

Profiling of proteins sampled by STAMP. Proteins sampled by STAMP [solubilization with 0.5% (wt/vol) DPS-B30 formulation with in situ 3 min sonication] from porcine skin and mucosal tissues including colon, nasal, and buccal mucosa were characterized. Mucosal tissues were procured from Sierra for Medical Science Inc. Tissues were frozen over dry ice immediately after harvesting and stored at −70 °C. STAMP-assisted sampling was performed by mounting the tissues on a Franz diffusion cell assembly according to the protocol described in the above sections.

Tissue homogenate samples were also prepared for comparative analysis. Tissues were cut into 2 cm × 2 cm pieces. Epidermal skin and mucosal membranes were gently scraped from the bulk tissues using a sharp scalpel. Care was taken to avoid scraping of the muscle and connective tissue underlying the mucosa. About 20 mg per cm^2 of the tissue was harvested and immediately added to sampling buffer (0.5% (wt/vol) DPS-B30 surfactant formulation prepared in saline; 1 mL per cm^2 of tissue). Tissues were completely homogenized using a mechanical homogenizer (Tissue Master-240, Omni International). An ice bath was used to avoid temperature increase during homogenization.

One-dimensional SDS electrophoresis was performed under reducing conditions with 7.5% polyacrylamide gels (Bio-Rad Laboratories) and protein samples were adjusted to a final concentration of 2% SDS and 2% mercaptoethanol prior to their loading. The protein migration patterns on fixed gels were stained with SYPRO® Ruby Protein Gel Stain reagent (170-3125, Bio-Rad Laboratories) and digitally imaged.

Gel densitometry. Gel images were processed and analyzed by ImageJ software. Specifically, gel image was background subtracted and an intensity line graph was generated for each protein lane of the gel. Line graphs were smoothened by five-point Savitsky–Golay function to remove white noise, and baseline corrected. For each resulting peak in the line graph (corresponding to a protein band in the lane), area under the peak was obtained as a measure of the amount of protein in the band. Fractional protein amount for each protein band was estimated by taking the ratio of the corresponding area under the peak and the total area under the line graph.

Quantification of localized transport regions in skin. Trypan Blue (T6146; Sigma-Aldrich) was used for visualizing the LTRs in the skin. Dye was mixed with the sampling buffer containing surfactants at a concentration of 5 mg/mL. Skin was exposed to the dye along with ultrasound application using the methods discussed above. Skin was then removed from the diffusion cell, rinsed in 30 mL of saline using a shaker operating at 700 rpm for 15 s. Skin was imaged using a digital camera (Optronics) within 10 min of ultrasound application. LTRs evident by dark blue spots on the skin were quantified by using an image analysis software—ImageJ. All the images were thresholded at a predetermined pixel intensity that allowed identification of LTRs in the images. Area occupied by LTRs was divided by the total area of skin exposed to ultrasound to calculate percent of the area occupied by LTRs.

FTIR spectroscopy measurements. Lysozyme solutions at a concentration of 5 mg/mL were prepared in deuterated phosphate-buffered saline with or without 0.5% (wt/vol) DPS-B30 surfactant formulation. Ultrasound was applied using methods previously described in the bioactivity measurement section. FTIR spectra were recorded by using a liquid-cell adaptor (0.2-mm spacer) in a Nicolet Magna 850 spectrometer setup at a resolution of 2 cm^{-1} and were averaged over 200 scans. Reference spectra were recorded under identical conditions but with corresponding buffer in the cell. Protein spectra were obtained by subtracting the corresponding reference spectrum. The spectra were

smoothed by five-point Savitsky–Golay function, baseline-corrected, and saved in the comma separated value format with Omnic software (Nicolet). Lysozyme's secondary structure was characterized by analyzing the amide I band (1,700–1,600 cm^{-1}) of the IR absorption spectrum. Amide I band was deconvoluted using Origin software and peaks corresponding to each secondary structure were assigned according to previously reported data (7, 8). Quantification was done by measuring the relative area under the peaks for each secondary structure.

Quantification of lysozyme aggregation with dynamic light scattering. Characterization of the size of lysozyme aggregates formed upon STAMP procedure was quantified by dynamic light scattering (Zetasizer Nano-ZS, Malvern Instruments). All protein solutions with or without surfactant formulations were prepared with dust-free saline (prepared by filtration through 0.2 μm PVDF syringe filters; Whatman Inc.). The samples were equilibrated at 25 °C for 2 min and the time-dependence autocorrelation function of each sample was acquired every 10 s, with 15 acquisitions for each run. The sample solution was illuminated by a 633-nm laser, and the intensity of light scattered at an angle of 173° was measured by an avalanche photodiode. All sizes are reported as hydrodynamic diameters in nm.

Profiling of lipids sampled by STAMP. STAMP samples were prepared in vitro from excised porcine skin and mucosal tissues including colon, nasal, and buccal mucosa. STAMP was carried out by mounting tissues on a Franz diffusion cell assembly, and using 0.5% (wt/vol) DPS-B30 surfactant formulation with a brief in situ 3-min sonication. Tissue homogenate samples were also prepared for comparative analysis by procedure outlined in the above section. Lipids from each sample were extracted with the Bligh-Dyer method (9). After evaporating the solvent under a stream of nitrogen, lipid weight was estimated by weighing and the lipids were reconstituted in 250 μL of chloroform/methanol (2:1) solvent for thin layer chromatography (TLC) analysis. Ten-centimeter-long aluminum-backed TLC plates coated with a 200-μm-thick layer of silica gel (60 Å) (Merck-5554/7, EMD Chemicals) were washed with chloroform/methanol (2:1), air dried, and 20 μL of each lipid extract was applied at 1 cm distance from the bottom of the plate. The chromatograms were developed successively with hexane (to 9 cm), toluene (to 9 cm), and hexane/ether/acetic acid (70:30:1, twice to 5 cm). Cholesteryl stearate (cholesteryl esters), triolein (triglycerides), oleic acid (free fatty acids), lanosterol, and cholesterol were spotted on TLC plates as reference standards. Lipids on the chromatographs were probed by charring them with 8% H_3PO_4 solution containing 10% wt/vol $CuSO_4$ and 5% vol/vol methanol, followed by slow heating at 180 °C in an oven until a good contrast was obtained. Cholesterol in samples obtained from mice skin in vivo was quantified with an enzymatic assay kit (catalog no. K603-100; BioVision Inc.). A colorimetric endpoint was obtained in the assay by utilizing the ability of cholesterol oxidase to oxidize cholesterol in the samples. A standard curve with known amounts of cholesterol was generated to quantify the cholesterol amount in samples.

Sampling of genomic DNA by STAMP. STAMP samples were prepared from excised porcine skin using 0.5% (wt/vol) DPS-B30 surfactant formulation and a brief in situ 3-min sonication. STAMP was carried out by mounting skin on Franz diffusion cell assembly as described in the above sections. The sonication probe was disinfected with 70% ethanol between experiments. As a comparative control, samples were obtained by swabbing the skin with cotton swabs (B4320115, BD Diagnostics). A sterile metal ring (area of 3.3 cm^2) was clamped onto the skin surface and sampling was restricted by swabbing skin enclosed within the ring. Swabs were soaked in sterile PBS and gently rubbed against skin surface for 20 s. Each swab was extracted with 1 mL of PBS solution for 1 h. Samples were also prepared by aggressively scraping the skin as previously described by Williamson and Kligman (10). Briefly, a sterile metal ring was firmly held against the skin surface and 1 mL of 0.1% (wt/vol) Triton X-100 in 0.075 M phosphate buffer, pH 7.9, was dispensed in it. The skin surface within the ring was rubbed firmly for 1 min with a Teflon cell scraper, and the resulting sample was collected. The procedure was repeated at the same skin site for two additional times and samples were pooled together.

Bacterial genome was purified from each sample by standard phenol-chloroform extraction method. Briefly, samples were first incubated in a solution consisting of 20 mM Tris at pH 8.0 (BP154, Fisher Scientific), 2 mM EDTA (BP120, Fisher Scientific), 1.2% Triton X-100 (BP151-100, Fisher Scientific), and 20 mg/mL lysozyme (62970, Sigma-Aldrich) for 30 min at 37 °C (as previously reported in ref. 11). Subsequently, samples were incubated for 3 h at 37 °C in a solution consisting of 0.1 mg/mL Proteinase K (P2308, Sigma-Aldrich), 0.5% (wt/vol) sodium lauryl sulfate (S529, Fisher Scientific), and 100 mM sodium chloride (BP358, Fisher Scientific). Genomic DNA was then extracted with an equal volume of phenol (P4557, Sigma-Aldrich), followed by extraction with phenol/chloroform/isoamyl alcohol, 25:24:1 (P2069, Sigma-Aldrich). The DNA was precipitated by incubation with ethanol and centrifugation for 20 min. The DNA pellets were washed twice with 70% ethanol, allowed to dry, and resuspended in 80 μL of tris buffer. To quantify the amount of bacteria in each sample, real-time quantitative PCR was performed based on an amplicon of the conserved 16S rRNA bacterial gene. Analysis of the 16S gene was performed on the iCycler PCR machine (Bio-Rad Laboratories) using optical grade 96-well plates. Bacterial 16S gene was amplified using forward primer 63F (5′-AGAGTTTGATCCTGGCTCAG-3′) and reverse primer 355R (5′-GACGGGCGGTGTGTRCA-3 (11, 12). For each sample, 10 μL of purified genomic DNA was mixed with 2 pmol of each primer and Platinum PCR Supermix (11784, Invitrogen) to a final reaction volume of 20 μL. Thermal cycling was set as follows: initial denaturation at 94 °C for 5 min, followed by 32 cycles of a 30-s 94 °C denaturation, 30-s annealing at 66 °C, and 30-s elongation at 72 °C, all followed by a final extension of 10 min at 72 °C. To calibrate number of bacteria in each sample, a standard curve was constructed by amplifying serial dilutions of genomic DNA from known quantities of *Escherichia coli* cells in 10 μL of tris buffer.

Additional experiments were conducted to evaluate the structural integrity of bacterial DNA under sonication stress of STAMP procedure. Bacterial culture of *E. coli* strain DH10α (18290-015, Invitrogen) were grown in Luria-Bertani (BP1426, Fisher Scientific) at 37 °C, 250 rpm. *E. coli* cells were quantified with a spectrophotometer (Biophotometer, Eppendorf), and a bacterial culture of 0.25×10^9 cells/mL was considered to correspond to an optical density absorbance value of 0.25 at a wavelength of 600 nm. Culture was harvested by centrifugation and the resulting pellet was suspended in either tris buffer (10 mM Tris-HCl, pH 7.9) or 0.5% (wt/vol) DPS-B30 surfactant formulation at a concentration of 10^9 cells/mL. One milliliter of cell suspension was placed in a sterilized sonication chamber (centrifuge tube #430290, Corning Inc.). Sonication (20 kHz, 2.4 W/cm^2, 50% duty cycle, 3 min; as used in STAMP procedure) was performed by lowering the probe transducer to a distance of 5 mm from the bottom of the chamber. After sonication, genome DNA was purified from each sample using the DNeasy DNA Extraction Kit (69504, Qiagen). The purified genomic DNA was resuspended in 400 μL of Buffer AE and subjected to electrophoresis for 90 min at 100 V in a 2% (wt/vol) Tris-acetate-EDTA-agarose gel. The gels were stained with SYBR Gold (S11494, Invitrogen) and visualized under UV light.

Allergy mouse model development. Six- to eight-week-old female BALB/CJ mice were purchased from Charles River Labs and maintained under pathogen-free conditions. All procedures performed on the mice were approved by the Institutional Animal Care and Use Committee of University of California, Santa Barbara, CA. Allergic reaction was induced in mice by an epicutaneous exposure protocol as described previously (13). Briefly, after anesthesia with 1.25–4% isofluorane in oxygen, the skin on the back of the mice was shaved and then tape stripped 10 times by a 3 M tape (3 M Health Care) to introduce a standardized skin injury. A gauze patch (1 cm × 1 cm) soaked with 100 μL of 0.1% OVA was placed on the back skin and secured with a breathable elastic cloth-based adhesive tape. The patches were kept affixed for 1 week. The whole experiment comprised a total of three 1-week exposures with a 2-week interval between each exposure week. All animal handling and maintenance protocols were approved by the Institutional Animal Care and Use Committee, University of California, Santa Barbara, CA.

1. Tezel A, Sens A, Tuchscherer J, Mitragotri S (2002) Synergistic effect of low-frequency ultrasound and surfactants on skin permeability. *J Pharm Sci* 91:91–100.
2. Tezel A, Sens A, Tuchscherer J, Mitragotri S (2001) Frequency dependence of sonophoresis. *Pharm Res* 18:1694–1700.
3. Chi EY, Krishnan S, Randolph TW, Carpenter JF (2003) Physical stability of proteins in aqueous solution: mechanism and driving forces in nonnative protein aggregation. *Pharm Res* 20:1325–1336.
4. Dong A, Prestrelski SJ, Allison SD, Carpenter JF (1995) Infrared spectroscopic studies of lyophilization- and temperature-induced protein aggregation. *J Pharm Sci* 84:415–424.
5. Carrion-Vazquez M, et al. (2000) Mechanical design of proteins studied by single-molecule force spectroscopy and protein engineering. *Prog Biophys Mol Biol* 74:63–91.
6. Stathopulos PB, et al. (2004) Sonication of proteins causes formation of aggregates that resemble amyloid. *Protein Sci* 13:3017–3027.
7. Byler DM, Susi H (1986) Examination of the secondary structure of proteins by deconvolved FTIR spectra. *Biopolymers* 25:469–487.
8. Fu K, et al. (1999) FTIR characterization of the secondary structure of proteins encapsulated within PLGA microspheres. *J Control Release* 58:357–366.
9. Bligh E, Dyer W (1959) A rapid method of total lipid extraction and purification. *Can J Biochem Physiol* 37:911–917.
10. Williamson P, Kligman A (1965) A new method for the quantitative investigation of cutaneous bacteria1. *J Invest Dermatol* 45:498–503.
11. Grice E, et al. (2008) A diversity profile of the human skin microbiota. *Genome Research* 18:1043–1050.
12. Castillo M, et al. (2006) Quantification of total bacteria, enterobacteria and lactobacilli populations in pig digesta by real-time PCR. *Vet Microbiol* 114:165–170.
13. Spergel JM, et al. (1998) Epicutaneous sensitization with protein antigen induces localized allergic dermatitis and hyperresponsiveness to methacholine after single exposure to aerosolized antigen in mice. *J Clin Invest* 101:1614–1622.

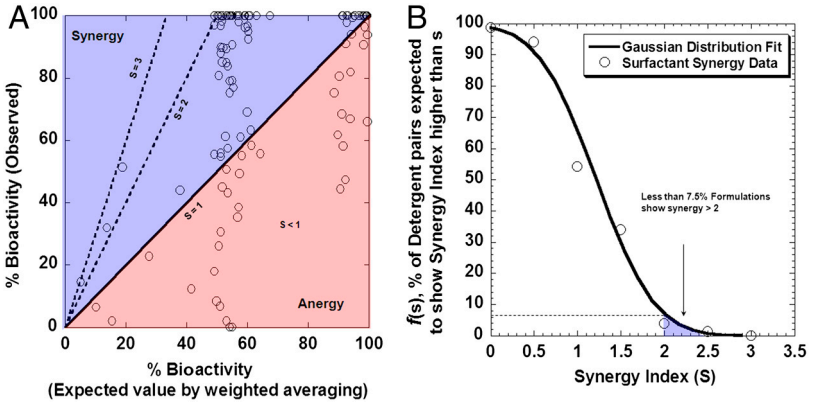

Fig. S1. (*A*) Synergistic interaction index (S) for each binary formulation was measured by plotting observed vs. expected bioactivity retention, and (*B*) a probability distribution was generated to assess the chances of achieving highly synergistic formulations.

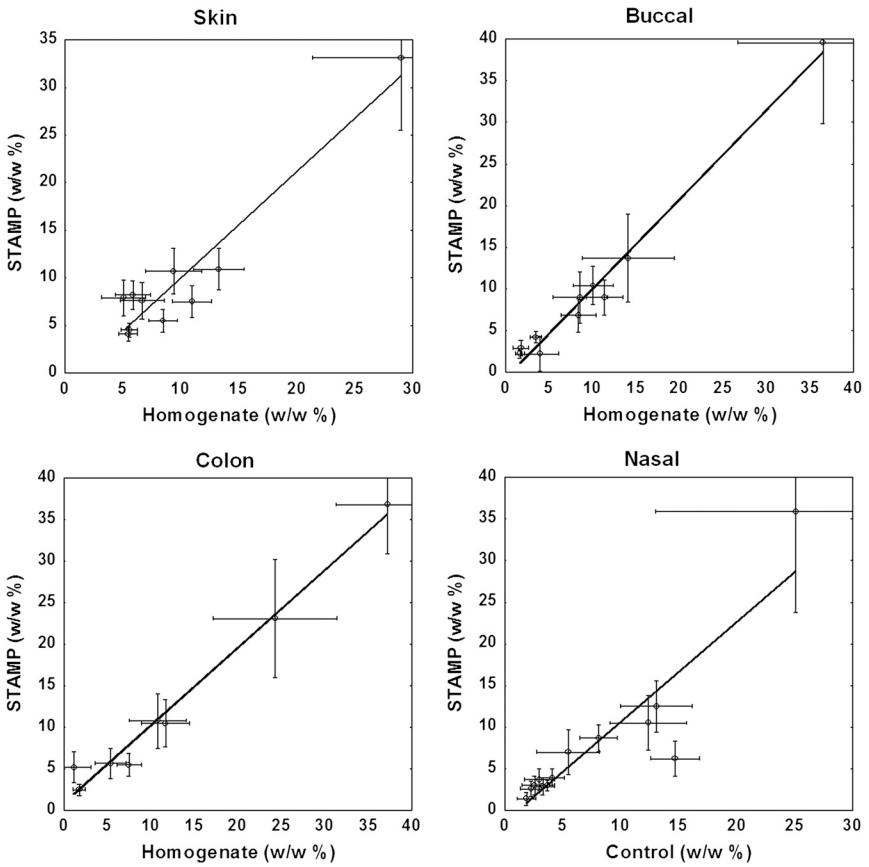

Fig. S2. Gel densitometry comparison of protein profiles in skin and mucosal tissues as measured in tissue homogenate, and in samples acquired by STAMP. Data reported in Table S1.

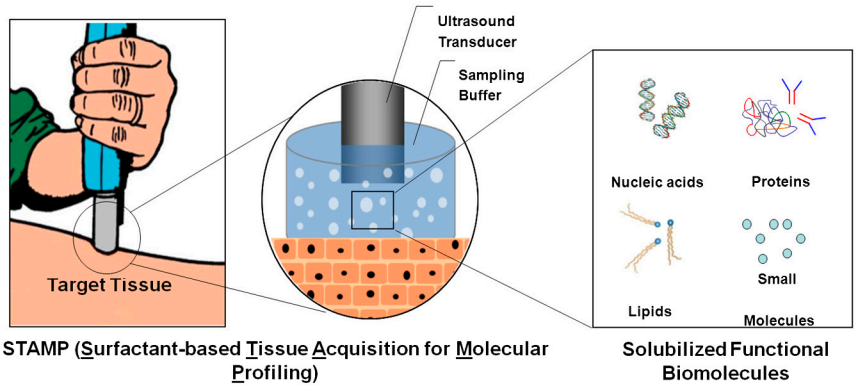

Fig. S3. Schematic conceptualizing STAMP-facilitated rapid one-step sampling of clinically relevant tissues in vivo. A handheld STAMP device may enable clinicians to rapidly and conveniently generate a liquefied tissue sample. STAMP sample constitutes a vast array of functional tissue biomolecules in similar proportions as they natively exist in the tissue. Onsite quantitative analysis of clinically relevant tissues with STAMP can sensitively determines subtle changes in the tissue chemistry permitting a patient-friendly method for localized tissue-based diagnosis.

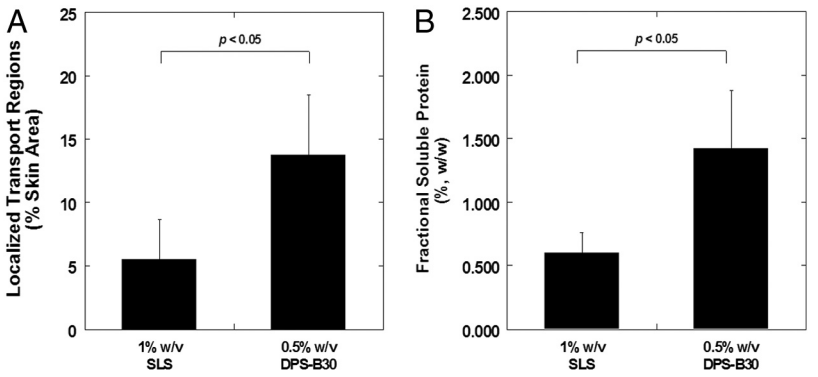

Fig. S4. (*A*) Enhanced solubilization potential of 0.5% (wt/vol) DPS-B30 was assessed by measuring the occurrence of LTRs in porcine skin during the STAMP procedure. Increase in fractional skin area covered by LTRs with DPS-B30 compared to 1% (wt/vol) SLS shows higher solubilization and increased sampling homogeneity. (*B*) DPS-B30 samples contained a higher amount of solubilized protein per total amount of protein sampled by STAMP from porcine skin.

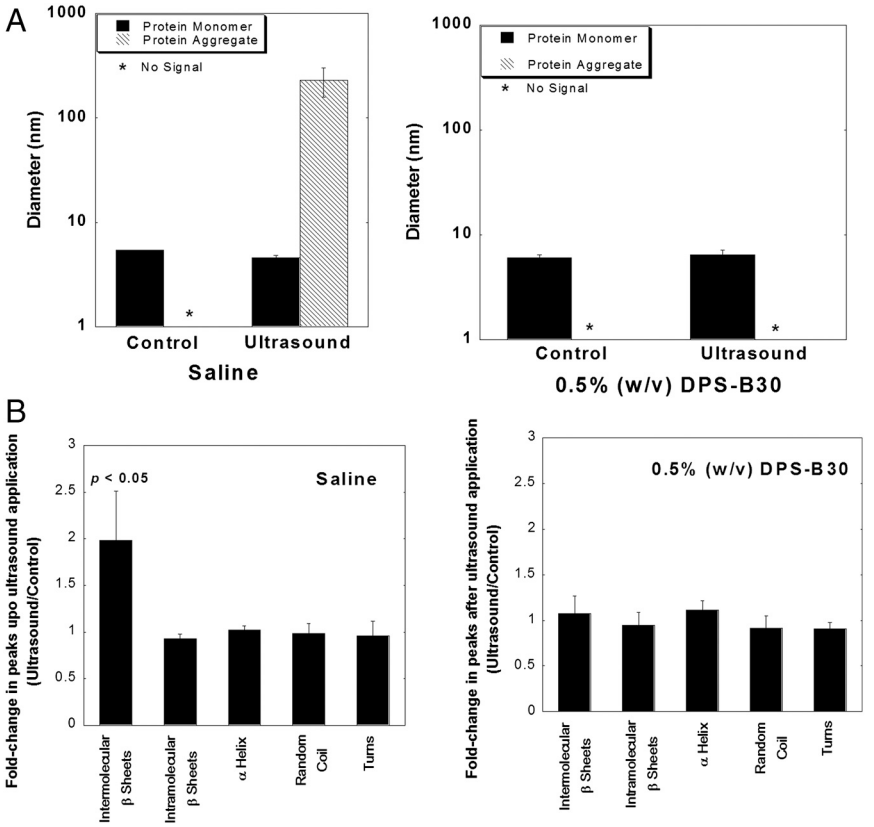

Fig. S5. (*A*) Effect of ultrasound on aggregation of lysozyme prepared in phosphate-buffered saline, or 0.5% (wt/vol) DPS-B30 surfactant formulation was studied using dynamic light scattering. Application of ultrasound to lysozyme in saline led to formation of aggregates. A subpopulation of monomers was retained, whose size was the same as that in the absence of ultrasound. The size of aggregates was dramatically higher than that of monomers. In case of DPS-B30, the micelle diameter was found to be 42–45 nm, which was not influenced by ultrasound. No aggregates were found when ultrasound was applied to lysozyme in DPS:B30. Control indicates nonsonicated samples. $N = 3$. (*B*) Effect of ultrasound on the secondary structure of lysozyme prepared in phosphate-buffered saline, or 0.5% (wt/vol) DPS-B30 surfactant formulation was studied using FTIR spectroscopy. Control indicates nonsonicated samples. $N = 3$.

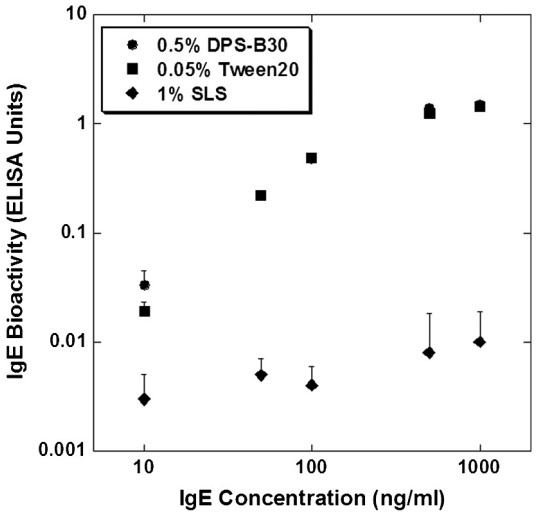

Fig. S6. Compatibility of the leading surfactant formulation—0.5% (wt/vol) DPS-B30 and other conventionally used surfactants (SLS and Tween20) with ELISA assay was assessed.

Table S1. Gel densitometry comparison of protein profiles in skin and mucosal tissues as measured in tissue homogenate, and in samples acquired by STAMP.

Protein band (MW, kDa)	Protein fraction (wt/wt %)	
	Homogenate	STAMP
Skin		
105–100	5.5 ± 1.0	4.8 ± 0.8
96–90	5.1 ± 1.2	7.9 ± 1.9
89–81	9.4 ± 2.2	10.7 ± 2.4
81–74	8.5 ± 1.5	5.5 ± 1.2
74–70	5.9 ± 1.1	8.2 ± 1.5
70–64	29.0 ± 6.8	33.1 ± 7.6
64–58	11.0 ± 2.2	7.5 ± 1.7
55–50	13.3 ± 2.6	10.9 ± 6.2
49–46	5.6 ± 1.3	4.5 ± 0.7
45–36	6.7 ± 1.3	7.6 ± 1.9
Buccal		
95–89	3.5 ± 0.8	4.2 ± 0.7
89–85	1.7 ± 0.3	2.2 ± 0.5
77–73	14.1 ± 2.7	13.7 ± 5.3
73–66	36.5 ± 4.4	39.6 ± 9.8
62–59	11.4 ± 2.6	9.0 ± 2.1
55–52	8.4 ± 1.9	6.8 ± 2.0
52–49	4.0 ± 0.7	2.2 ± 2.1
49–43	10.1 ± 2.1	10.4 ± 2.3
42–39	1.8 ± 0.4	2.9 ± 0.9
39–35	8.6 ± 1.7	9.0 ± 3.1
Colon		
96–87	7.5 ± 1.9	5.5 ± 1.4
77–73	10.8 ± 2.9	10.8 ± 3.3
72–67	24.3 ± 4.5	23.1 ± 7.1
67–57	37.2 ± 13.7	36.8 ± 5.9
57–53	1.2 ± 0.5	5.2 ± 1.9*
49–43	5.4 ± 1.3	5.7 ± 1.8
43–39	1.8 ± 0.6	2.5 ± 0.7
39–35	11.7 ± 4.5	10.5 ± 2.8
Nasal		
102–96	5.5 ± 1.4	7.0 ± 2.7
94–90	4.1 ± 1.0	3.9 ± 1.1
90–85	2.6 ± 0.4	3.0 ± 1.1
83–78	3.3 ± 0.7	2.9 ± 1.0
77–73	13.1 ± 4.7	12.5 ± 3.1
72–66	25.1 ± 8.3	35.9 ± 12.1
63–59	12.4 ± 3.9	10.5 ± 3.3
59–54	14.7 ± 4.4	6.2 ± 2.1*
54–50	3.7 ± 0.8	3.0 ± 0.6
50–46	2.3 ± 0.9	2.6 ± 0.9
43–41	3.0 ± 1.9	3.7 ± 1.3
40–37	8.1 ± 3.2	8.7 ± 1.6
37–34	1.9 ± 0.9	1.4 ± 0.8

*Significant difference between amount of protein sampled by STAMP and protein present in tissue homogenate ($p < 0.05$, student's t test). $N = 3$.